

# Domain Coarsening in Electroconvection

Lynne Purvis

Michael Dennin

*Department of Physics and Astronomy*

*University of California at Irvine*

*Irvine, CA 92697-4575.*

(February 7, 2020)

We report on experimental measurements of the growth of regular domains evolving from an irregular pattern in electroconvection. The late-time growth of the domains is consistent with the size of the domains scaling as  $t^n$ . We use two different measurements of the domain size: the structure factor and the domain wall length. Measurements using the structure factor are consistent with  $t^{1/5}$  growth, in agreement with simulations. Measurements using the domain wall length are consistent with  $t^{1/4}$  growth. We show that one source of this discrepancy is that the distribution of local wavenumbers is approximately independent of the domain size.

47.54+r,64.60.Cn

There are many situations where a system experiences a rapid change of an external parameter, or quench, such that the state of the system after the quench is not an equilibrium or steady-state phase. Domains of the new equilibrium phase form, and the subsequent growth of these domains, or *coarsening*, is often characterized by a single scale size for the domains that follows a power-law growth. There has been a great deal of both theoretical and experimental study of this process for systems where both the initial state prior to the quench and final state after the quench are thermodynamic equilibrium states at finite temperature [1]. In this paper, we are interested in the analogous process for spatially extended systems that are driven out of equilibrium. For such systems, neither the initial nor the final state is in thermodynamic equilibrium; however, they are steady-states of the system. For the purposes of this paper, the first situation will be referred to as a *thermodynamic system* and the second situation as a *driven system*. For driven systems, studies of model equations suggest power-law scaling of the late-time domain growth; however, the value of the growth exponent is dependent on the measurement scheme [2–4]. Experimentally, the coarsening of random patterns after a ramp in the control pattern has been studied, but growth exponents for domain size were not measured [5].

In spatially extended systems that are driven out of equilibrium, there is generally a transition from a uniform state to a periodic, or “stripe”, state at a critical value  $R_c$  of the external control parameter  $R$  [6]. For these systems, a quench corresponds to a rapid change of  $R$ .

For values reasonably close to  $R_c$ , these systems are often well described by model equations that are similar to, and in some cases identical to, the equations used to study coarsening in thermodynamic systems [6]. Therefore, one might expect similar scaling of the late-time coarsening of domains for the two classes of systems. However, in a driven system, there is generally no equivalent of a free-energy that governs the growth of the domains, and the periodic structure complicates the dynamics. Therefore, the question of how the ordering proceeds in driven systems is one of great interest.

Simulations of various forms of the Swift-Hohenberg equation have been used to study quenches from values of  $R < R_c$  to  $R > R_c$  [2–4]. The subsequent growth and ordering of domains is characterized both by the structure factor ( $S(k)$ ) [2–4] and by a correlation function based on the orientation of the stripes [3,4]. Reference [3] considers both potential and nonpotential dynamics, and Ref. [4] only considers the potential case. In both cases,  $S(k)$  suggests a length scale that grows as  $t^{1/5}$  [3,4]. In contrast, the growth exponent determined from the orientational correlation function is consistent with 1/4 [3,4] for potential dynamics and is consistent with 1/2 [3] for nonpotential dynamics. There is no explanation of the discrepancy between the  $S(k)$  and orientational correlation function measurements; however, the length scales determined by these measures do not have the same immediate interpretation [4].

We have made experimental measurements of coarsening in a driven system. Using  $S(k)$ , we observe growth exponents that are consistent with 1/5. This method combines two measures of the domain growth in a non-trivial fashion: the domain size and the distribution of local wavenumbers. As a direct measure of domain growth, we consider the total domain wall length. These results are consistent with a growth exponent of 1/4. Our direct measurement of the distribution of local wavenumbers shows that this distribution is essentially independent of time. This suggests that at least two length scales, domain size and local wavenumber, are needed to describe the domain growth. As  $S(k)$  measures a combination of domain size and local wavenumber, it is not surprising that the  $S(k)$  growth exponents differ from those determined by methods that are independent of the local wavenumber, such as the orientational correlation func-

tions used in Ref. [3] and [4].

The experimental system is electroconvection in a nematic liquid crystal [7]. A nematic liquid crystal is a fluid in which the molecules align on average along a particular axis, referred to as the director [8]. For electroconvection, the liquid crystal is placed between two glass plates with the director aligned parallel to the plates and along a single axis. The liquid crystal is doped with ionic impurities. An ac voltage is applied perpendicular to the plates. Above a critical value of the applied voltage  $V_c$ , there is a transition to a state that consists of convection rolls with a corresponding periodic variation of the director and charge density.

We studied *oblique rolls*, i.e. patterns that have a nonzero angle  $\theta$  between the wavevector and the alignment of the undistorted director. Oblique rolls with the same wavenumber  $k$  but at  $\theta$  and  $-\theta$  are degenerate and are called zig and zag rolls, respectively. The initial transition in this system is to a pattern that consists of the superposition of four modes: right- and left-traveling zig and zag rolls. The interaction of these four modes leads to irregular spatial and temporal variations of the amplitudes of each of the modes [9], i.e. spatiotemporal chaos [6,10]. For traveling rolls, a sufficiently large modulation of the amplitude of the applied voltage at twice the intrinsic frequency of the pattern stabilizes standing rolls [11–13]. For our system, either standing zig or standing zag rolls are stabilized, and the stabilized pattern exhibits regular temporal dynamics [14]. In our experiments, a quench corresponded to a rapid change of the modulation amplitude at a fixed value of the  $V_{rms}$ . As standing waves can be stabilized both below and above  $V_c$ , two types of quenches are possible. Below  $V_c$ , the dynamics of the standing waves are potential [15], and above  $V_c$ , they are nonpotential [16]. Therefore, based on the results of Ref. [3], we expected two different growth exponents. Also, below  $V_c$ , domains of standing zig and zag rolls must first form before the system coarsens, as the initial state is spatially uniform. This process is illustrated in Fig. 1(a) - (d). Above  $V_c$ , domains of zig and zag rolls are already present after the quench, and the coarsening proceeds from this initial distribution. This process is illustrated in Fig. 1(e) - (h).

The details of the experimental apparatus are described in Ref. [14]. We used commercial cells [17] with a thickness of  $23 \mu\text{m}$ . The electrodes covered a  $1 \text{ cm}^2$  area in the center of the cell, which had an area of  $6.25 \text{ cm}^2$ . The sample was held in a temperature control stage, and the temperature was maintained at  $50.0 \pm 0.002 \text{ }^\circ\text{C}$ . The patterns were observed using a modified shadowgraph setup that is described in detail in Ref. [18]. Light polarized perpendicular to the undistorted director entered the sample from below. A quarter wave plate with its optical axis at  $45^\circ$  to the polarizer was placed above the sample. This was followed by a second polarizer aligned at  $85^\circ$  with respect to the first one. Finally, the image

was observed using a CCD camera. This setup effectively eliminates the well-known nonlinear effects in the shadowgraph image [19] that were found to interfere with our image analysis techniques.

An ac voltage was applied across the sample of the form  $V(t) = [V_o + V_m \sin(\omega_m t)] \sin(\omega_d t)$ . There are two relevant dimensionless control parameters:  $\epsilon = (V_o/V_c)^2 - 1$  and  $b = V_m/V_c$ . Here  $V_c$  is the critical voltage for the onset of a pattern when  $V_m = 0$ . The drive frequency was  $\omega_d/2\pi = 25 \text{ Hz}$ . There was a small, linear drift in  $V_c$ ; therefore, before and after each quench,  $V_c$  and  $\omega_h$  were determined. The typical values were  $V_c = 15 V_{rms}$  and  $\omega_h/2\pi = 0.5 \text{ Hz}$ .

The system was equilibrated at  $b = 0$  and either  $\epsilon = -0.03$  or  $\epsilon = 0.03$  for five minutes. For  $\epsilon = -0.03$ , the transition to standing waves occurs at  $b = 0.03$  [14]. For  $\epsilon = 0.03$ , the transition is at  $b = 0.013$  [14]. The two quenches discussed in detail are for  $\epsilon = -0.03$  with a jump in  $b$  from 0 to 0.05 and for  $\epsilon = 0.03$  with a jump in  $b$  from 0 to 0.04. For both of these quenches,  $\omega_m = 2\omega_h$ , where  $\omega_h$  is the frequency of the pattern at onset, the Hopf frequency. A third quench was done at  $\epsilon = 0.03$  for  $\omega_m = 2.1\omega_h$ . Immediately after the jump in  $b$ , we took a series of 128 images. The framegrabber was triggered by the signal generating the ac voltage, and the images were always taken at  $T/4$ , where  $T$  is the period of the modulation. An image was taken every  $5^{th}$  cycle of the modulation, or roughly once every 5 seconds. Because we needed to resolve the individual rolls to distinguish the zig and zag domains, we were only able to observe a  $1.35 \text{ mm}$  by  $1.35 \text{ mm}$  section of the sample. At the end of a typical time series, the domain size was on the order of our observation window. Given the size of our window relative to the entire sample, we were not limited by finite size effects. Unless otherwise noted, time is scaled by the director relaxation time, which for our system is  $0.2 \text{ s}$ . For  $\epsilon = 0.03$ , we performed 20 quenches, and for  $\epsilon = -0.03$ , we performed 18 quenches. The domain wall length,  $S(k)$ , and the local wavenumber distribution were computed for each image in the time series for a given quench. The values at each time step were averaged over all the quenches for a given  $\epsilon$ , and these averaged values were used to compute the growth exponents. The values of the growth exponents did not change significantly after averaging 10 runs.

If a single scale length is sufficient to describe the domain growth, both the total domain wall length and the width of the power spectrum would exhibit the same growth exponent. However, as mentioned, the structure factor contains information about the range of local wavenumbers within a domain. Therefore, we measured the local wavenumber using the method described in Ref. [20] as an independent check on the scaling of the wavenumber spread. Briefly, the method described in Ref. [20] involves calculating the x-component of  $k$  using  $|k_x|^2 = -[\partial_x^2 u(\mathbf{x})]/u(\mathbf{x})$ , with a similar calculation for

the y-component. Here  $u(\mathbf{x})$  is the image of the pattern. For the results reported here, only the central 0.82 mm by 0.82 mm region of the image was considered in the determination of the spread  $\Delta k$  of the magnitude  $k$  of the local wavevector  $\mathbf{k}$ . We defined  $\Delta k$  as the square root of the second moment of the distribution of  $k$  about  $k_{ave}$ .

To determine the normalized domain-wall length  $L$ , the local wavenumber was used to distinguish the zig and zag rolls by considering the sign of  $[\partial_{xy}u(\mathbf{x})]/u(\mathbf{x})$ . Regions with a negative value of this ratio corresponded to zig rolls and were assigned a grayscale of 0. Regions with a positive value of this ratio corresponded to zag rolls and were assigned a grayscale value of 255. The resulting image was smoothed by convolving the image with a Gaussian ball with a radius of 2 pixels. This smoothing produced an image in which the regions of a domain wall had a value close to 128 due to the mixture of zig and zag rolls. A second threshold was applied to the image such that zig regions had a value of 0, domain walls a value of 128, and zag rolls a value of 255. The domain wall “length” was taken to be the total number of pixels of value 128 normalized by the total number of pixels in the image. Images from a typical sequence, after processing, are shown in Fig. 1 for two different quenches.

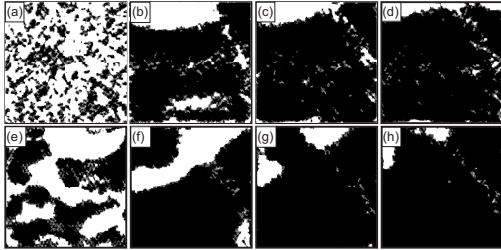


FIG. 1. Processed images illustrating the domain growth for a quench at  $\epsilon = -0.03$  (images (a) - (d)) and for a quench at  $\epsilon = 0.03$  (images (e) - (h)). The images cover an area of 1.35 mm by 1.35 mm, and the processing method is described in detail in the text. The black regions are areas of zig rolls, and the white areas are regions of zag rolls. Image (a)/(f) was taken 5 s after the quench, and the subsequent images are all 160 s apart.

The domain size is related to the inverse width of the relevant peak in the structure factor  $S(k)$ . To determine this width, we used the same method as described in Ref. [3]. First, the structure factor (the square of the Fourier transform) was averaged over all angles. The relevant peak in the resulting  $S(k)$  was fit to a Lorentzian squared, and the width  $\delta k$  was defined as the half width at half height. This method ensured that our results are directly comparable to Ref [3].

The averaged results for both quenches are summarized in Figs. 2 and 3. Figures 2a and 2b show the results for the domain wall length  $L$  for the  $\epsilon = -0.03$  and  $\epsilon = 0.03$  quenches, respectively. Here  $\log(L)$  is plotted

versus  $\log(t)$ . For the quench at  $\epsilon = 0.03$ , the behavior is consistent with power law scaling essentially immediately after the quench. For  $\epsilon = -0.03$ , the system is not consistent with power law scaling until  $\log(t) \approx 2.5$ . This difference is reasonable given that the domains must first form for the quench at  $\epsilon = -0.03$ . Also, the scaling occurs in both systems at roughly the same scale size for the domains,  $\log(L) \approx -1.2$ . The decay of the domain-wall length is consistent with scaling as  $t^{-1/4}$ . The solid line in Fig. 2a is a fit over the range  $2.5 < \log(t) < 3.5$  and has a slope of  $-0.24$ . The solid line in Fig. 2b is a fit over the range  $2.0 < \log(t) < 3.2$  and also has a slope of  $-0.24$ .

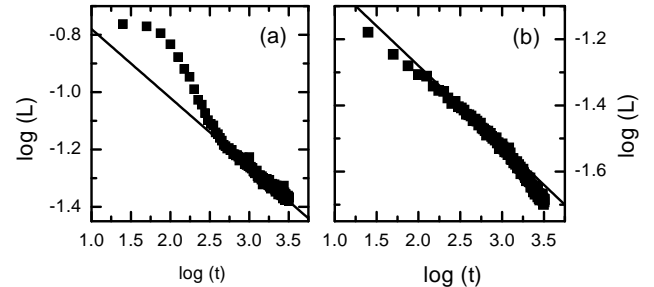


FIG. 2. This shows a plot of  $\log(L)$  versus  $\log(t)$ . Here  $L$  is the total length of the domain wall in the region of study. Plot (a) is for the quench at  $\epsilon = -0.03$ , and plot (b) is for the quench at  $\epsilon = 0.03$ . The solid lines are linear fits to the data. The line in (a) has a slope of  $-0.240 \pm 0.004$ , and the line in (b) has a slope of  $-0.243 \pm 0.003$ .

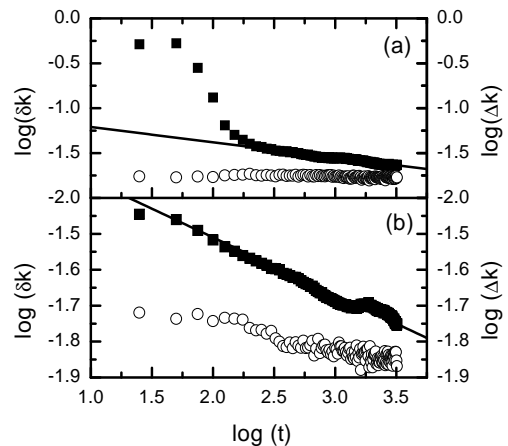


FIG. 3. This shows a plot of  $\log(\delta k)$  versus  $\log(t)$  using the left hand axis and solid symbols, and a plot of  $\log(\Delta k)$  versus  $\log(t)$  using the right hand axis and open symbols. Plot (a) is for the quench at  $\epsilon = -0.03$ , and plot (b) is for the quench at  $\epsilon = 0.03$ . The solid lines are linear fits to the solid data. The line in (a) has a slope of  $-0.170 \pm 0.003$ , and the line in (b) has a slope of  $-0.165 \pm 0.002$ .

Figures 3a and 3b show  $\log(\delta k)$  and  $\log(\Delta k)$  versus  $\log(t)$  for the quenches at  $\epsilon = -0.03$  and  $\epsilon = 0.03$ , re-

spectively. Again, we observe behavior consistent with power-law scaling almost immediately for  $\epsilon = 0.03$  and at later times for  $\epsilon = -0.03$ , with the scaling setting in for both quenches at approximately the same domain size. For both quenches, the scaling of  $\delta k(t)$  is consistent with  $t^{-1/5}$  decay, as found in simulations [3,4]. For  $\epsilon = -0.03$ , the solid line is a fit to the data over the region  $2.5 < \log(t) < 3.5$  and has a slope of -0.17. For  $\epsilon = 0.03$ , the solid line is a fit to the data over the region  $2.0 < \log(t) < 3.2$  and has a slope of -0.16. However, for both cases, the variation in the local wavenumber  $\Delta k$  accounts for a significant fraction of  $\delta k$  in the possible scaling regime, and it is roughly constant in time. Clearly,  $\delta k$  is not an accurate measure of the growth of the domain size. Instead, it is a complicated convolution of the domain size and  $\Delta k$ . This result will hold true for most systems in which the domains are composed of stripes.

One striking result was the measurement of a growth exponent of 1/4 for both  $\epsilon < 0$  and  $\epsilon > 0$ . For  $\epsilon > 0$ , the nonpotential case, we expected an exponent of 1/2 [3]. However, the dispersion relation for the system determines the average wavenumber  $k_{ave}$ . For  $\omega_m = 2\omega_h$ ,  $k_{ave} = k_o$ , where  $k_o$  is the critical wavenumber that appears in the Swift-Hohenberg equation. An analysis of the Swift-Hohenberg equation for patterns with  $k = k_o$  suggests that there is a long-time transient regime for which the growth exponent is 1/4 [2,4]. To vary  $k_{ave}$ , we performed a quench at  $\omega_m = 2.1\omega_h$ , for which  $k_{ave} = 1.07k_o$ . The quench was at  $\epsilon = 0.03$  to a value of  $b = 0.04$ . We still observed a growth exponent consistent with 1/4 for  $L$ . However, the average wavenumber exhibited a slow approach to a steady state (see Fig. 4), suggesting that this growth exponent also corresponds to a transient regime.

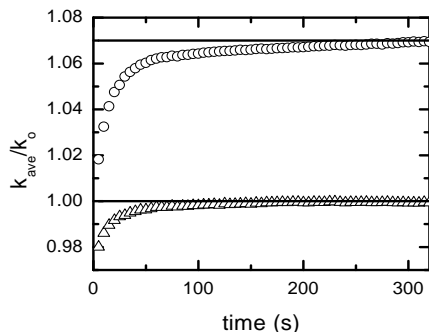


FIG. 4. This shows a plot of  $k_{ave}/k_o$  versus time. The triangles are for the quench at  $\epsilon = 0.03$  with  $\omega_m = 2.0\omega_h$ , and the circles are for the quench at  $\epsilon = 0.03$  with  $\omega_m = 2.1\omega_h$ . The lines are a guide to the eye.

In summary, we have shown that the growth of domains in our system is characterized by two length scales: one for the domain size and one for the local wavenum-

ber. The domain size exhibits behavior consistent with a growth exponent of 1/4, and the local wavenumber is independent of time. These two length scales result in the measurement of a growth exponent of 1/5 as determined by the structure factor, consistent with simulations of the Swift-Hohenberg equation. For the nonpotential case, there is strong evidence that we are only able to study a long-time transient. By exploiting the optical properties of the zig and zag rolls, we plan to study the domain growth without resolving the individual rolls. Therefore, larger regions of the sample and longer times will be studied. This opens the possibility of observing a crossover to  $t^{1/2}$  growth. Finally, a detailed study of the effect of the selected wavenumber is outside the scope of this letter, but it will be the subject of future work.

The authors acknowledge funding from NSF grant DMR-9975479. L. Purvis was supported by NSF Research Experience for Undergraduates grant PHY-9988066. M. Dennin would like to thank Michael Cross and Herman Riecke for useful discussions.

- 
- [1] A. J. Bray, *Advances in Physics* **43**, 357 (1994).
  - [2] K. R. Elder, J. Vinals, and M. Grant, *Phys. Rev. Lett.* **68**, 3024 (1992).
  - [3] M. C. Cross and D. I. Meiron, *Phys. Rev. Lett.* **75**, 2152 (1995).
  - [4] J. J. Christensen and A. J. Bray, *Phys. Rev. E* **58**, 5364 (1998).
  - [5] C. W. Meyer, G. Ahlers, D. S. Cannell, *Phys. Rev. A* **44**, 2514 (1991).
  - [6] For reviews of pattern formation, see M. C. Cross and P. C. Hohenberg, *Rev. Mod. Phys.* **65**, 851 (1993), and J. P. Gollub and J. S. Langer, *Rev. Mod. Phys.* **71**, s396 (1999).
  - [7] Review articles on electroconvection can be found in I. Rehberg, B. L. Winkler, M. de la Torre Juárez, S. Rasenat, and W. Schöpf, *Festkörperprobleme* **29**, 35 (1989); S. Kai and W. Zimmermann, *Prog. Theor. Phys. Suppl.* **99**, 458 (1989); and L. Kramer and W. Pesch, *Annu. Rev. Fluid Mec.* **27**, 515 (1995).
  - [8] P. G. de Gennes, *The Physics of Liquid Crystals* (Clarendon Press, Oxford, 1974); S. Chandrasekhar, *Liquid Crystals* (Cambridge University Press, Cambridge, England, 1992).
  - [9] M. Dennin, G. Ahlers, and D. S. Cannell, *Science* **272**, 388 (1996).
  - [10] For a recent review of experimental examples of spatiotemporal chaos, see G. Ahlers, *Physica A* **249**, 18 (1998).
  - [11] H. Riecke, J. D. Crawford, and E. Knobloch, *Phys. Rev. Lett.* **61**, 1942 (1988).
  - [12] D. Walgraef, *Europhys. Lett.* **7**, 485 (1988).
  - [13] I. Rehberg, S. Rasenat, J. Fineberg, M. de la Torre Juárez, and V. Steinberg, *Phys. Rev. Lett.* **61**, 2449

(1988).

- [14] M. Dennin, Phys. Rev. E, (2000).
- [15] H. Riecke, Europhys. Lett. **11**, 213 (1990).
- [16] H. Riecke, private communication.
- [17] E.H.C. CO., Ltd., 1164 Hino, Hino-shi, Tokyo, Japan.
- [18] H. Amm, R. Stannarius, and A. G. Rossberg, Physica D **126**, 171 (1999).
- [19] S. Rasenat, G. Hartung, B. L. Winkler, and I. Rehberg, Experiments in Fluids **7**, 412 (1989).
- [20] D. A. Egolf, I. V. Melnikov, and E. Bodenschatz, Phys. Rev. Lett. **80**, 3228 (1998).